The Astrophysical Journal Letters, 735:L37 (7pp), 2011 July 10 doi:10.1088/2041-8205/735/2/L37

EVIDENCE FOR MAGNESIUM ISOTOPE HETEROGENEITY IN THE SOLAR PROTOPLANETARY DISK

Kirsten K. Larsen[1], Anne Trinquier[1], Chad Paton[1], Martin Schiller[1], Daniel Wielandt[1], Marina A. Ivanova[2], James N. Connelly[1], Åke Nordlund[1,3], Alexander N. Krot[1,4], and Martin Bizzarro[1]
[1] Centre for Star and Planet Formation, Natural History Museum of Denmark, University of Copenhagen, Copenhagen DK-1350, Denmark
[2] Vernadsky Institute of Geochemistry and Analytical Chemistry, Moscow 119991, Russia
[3] Niels Bohr Institute, University of Copenhagen, Copenhagen DK-1350, Denmark
[4] Hawai'i Institute of Geophysics and Planetology, University of Hawai'i at Manoa, HI 96822, USA
Received 2011 April 8; accepted 2011 June 6; published 2011 June 21

ABSTRACT

With a half-life of 0.73 Myr, the ^{26}Al-to-^{26}Mg decay system is the most widely used short-lived chronometer for understanding the formation and earliest evolution of the solar protoplanetary disk. However, the validity of ^{26}Al–^{26}Mg ages of meteorites and their components relies on the critical assumption that the canonical ^{26}Al/^{27}Al ratio of $\sim 5 \times 10^{-5}$ recorded by the oldest dated solids, calcium–aluminium-rich inclusions (CAIs), represents the initial abundance of ^{26}Al for the solar system as a whole. Here, we report high-precision Mg-isotope measurements of inner solar system solids, asteroids, and planets demonstrating the existence of widespread heterogeneity in the mass-independent ^{26}Mg composition (μ^{26}Mg*) of bulk solar system reservoirs with solar or near-solar Al/Mg ratios. This variability may represent heterogeneity in the initial abundance of ^{26}Al across the solar protoplanetary disk at the time of CAI formation and/or Mg-isotope heterogeneity. By comparing the U–Pb and ^{26}Al–^{26}Mg ages of pristine solar system materials, we infer that the bulk of the μ^{26}Mg* variability reflects heterogeneity in the initial abundance of ^{26}Al across the solar protoplanetary disk. We conclude that the canonical value of $\sim 5 \times 10^{-5}$ represents the average initial abundance of ^{26}Al only in the CAI-forming region, and that large-scale heterogeneity—perhaps up to 80% of the canonical value—may have existed throughout the inner solar system. If correct, our interpretation of the Mg-isotope composition of inner solar system objects precludes the use of the ^{26}Al–^{26}Mg system as an accurate early solar system chronometer.

Key words: meteorites, meteors, meteoroids – protoplanetary disks

1. INTRODUCTION

The presence and initial abundances of short-lived radionuclides (e.g., ^{26}Al, ^{41}Ca, ^{53}Mn, ^{60}Fe, ^{182}Hf) in the solar system are widely used to understand the timescales of processes in the early solar system and to deduce the astrophysical environment where our Sun formed (McKeegan & Davis 2003; Goswami 2004). These radionuclides are believed to have a nucleosynthetic, stellar origin and have been either inherited from the interstellar medium or injected into the protosolar molecular cloud prior to or contemporaneously with its collapse (Sahijpal & Goswami 1998). If ^{26}Al that decays to ^{26}Mg with a half-life of 0.73 Myr was uniformly distributed in the solar system, it potentially provides a precise relative chronometer for early solar system processes (e.g., Lee et al. 1977; Russell et al. 1996; Galy et al. 2000; Bizzarro et al. 2004).

Uniform distribution of ^{26}Al in the solar system with the so-called *canonical* initial ^{26}Al/^{27}Al ratio of $(5.23 \pm 0.13) \times 10^{-5}$ (Jacobsen et al. 2008) has been inferred from Mg-isotope measurements of primitive meteorites and their components (Thrane et al. 2006; Villeneuve et al. 2009), and from the concordancy between ^{26}Al–^{26}Mg and ^{207}Pb–^{206}Pb ages obtained on the same chondritic components, namely calcium–aluminium-rich inclusions (CAIs) and chondrules (Amelin et al. 2002; Connelly et al. 2008a). However, the resolution required to unequivocally rule out ^{26}Al heterogeneity has been unattainable by state-of-the-art Mg-isotope measurements. For example, accepting the initial ^{26}Al/^{27}Al ratio [$(^{26}\mathrm{Al}/^{27}\mathrm{Al})_0$] of 5.23×10^{-5} (Jacobsen et al. 2008), the amount of radiogenic ^{26}Mg resulting from the in situ decay of ^{26}Al [$\mu^{26}\mathrm{Mg}^* = ((^{26}\mathrm{Mg}/^{24}\mathrm{Mg})_{\mathrm{sample}}/(^{26}\mathrm{Mg}/^{24}\mathrm{Mg})_{\mathrm{standard}} - 1) \times 10^6$] in a reservoir with solar ^{27}Al/^{24}Mg ratio of 0.101 is only 38 ppm (Figure 1(a)). As a result, an uncertainty of ±10 ppm in measurements of the μ^{26}Mg* value in samples of meteorites with an approximately solar ^{27}Al/^{24}Mg ratio could conceal a heterogeneity of up to 50% in $(^{26}\mathrm{Al}/^{27}\mathrm{Al})_0$ (Figure 1(a)). Moreover, the recent discovery of variable U-isotope compositions of early solar system solids (Brennecka et al. 2010) clouds the accuracy of ^{207}Pb–^{206}Pb ages used to infer consistency with the ^{26}Al–^{26}Mg chronometer.

To understand the degree of ^{26}Al homogeneity in the solar protoplanetary disk, we have developed analytical protocols allowing the measurements of the μ^{26}Mg* value and ^{27}Al/^{24}Mg ratios in meteorites by high-resolution multi-collector inductively coupled plasma source mass spectrometry (HR-MC-ICPMS) with an external reproducibility of 2.5 ppm and 0.5%, respectively (Bizzarro et al. 2011; Paton et al. 2011). Using these techniques, we report bulk Mg-isotope and ^{27}Al/^{24}Mg ratio measurements of a representative suite of inner solar system objects, including CAIs and amoeboid olivine aggregates (AOAs) from the reduced CV (Vigarano type) chondrite Efremovka as well as a number of primitive and differentiated meteorites.

2. μ^{26}Mg* HETEROGENEITY IN BULK SOLAR SYSTEM RESERVOIRS

The mineralogy, petrology, and oxygen isotopic compositions of CAIs and AOAs from primitive chondrites suggest a close genetic relationship between these objects. CAIs are formed by evaporation, condensation, and, in some cases, subsequent melting of refractory dust (MacPherson 2003). The CAI-forming processes occurred in an ^{16}O-rich ($\Delta^{17}\mathrm{O} \sim -25‰$) region with high ambient temperature, at or above the condensation

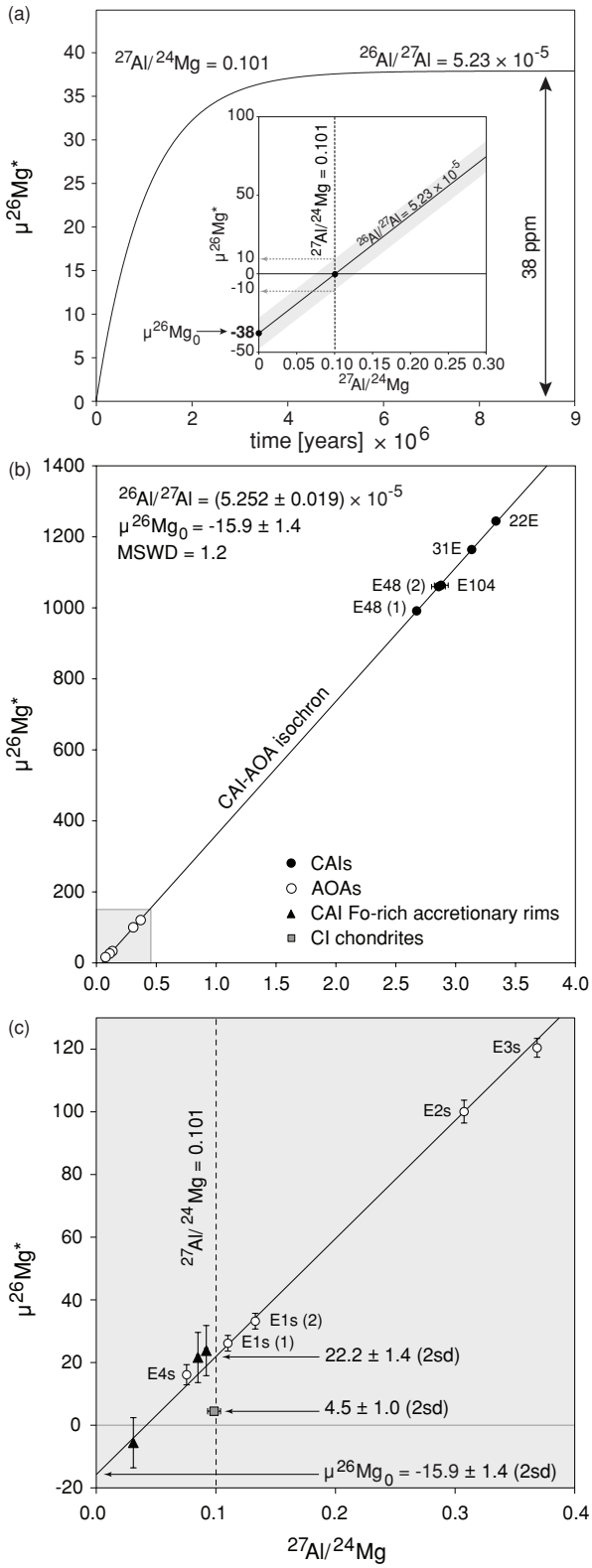

Figure 1. Al–Mg evolution diagrams. (a) Assuming a canonical $(^{26}Al/^{27}Al)_0$ of 5.23×10^{-5}, the amount of radiogenic ^{26}Mg resulting from the in situ decay of ^{26}Al ($\mu^{26}Mg^*$) in a reservoir with solar $^{27}Al/^{24}Mg$ is only 38 ppm. Thus, the intercept of an ^{26}Al–^{26}Mg isochron with the canonical $^{26}Al/^{27}Al$ ratio should be −38 ppm, assuming ^{26}Al homogeneity (inset). (b) Al–Mg isochron for bulk AOAs and CAIs from the reduced chondrite Efremovka. (c) The bulk Efremovka CAI–AOA isochron intercepts the solar $^{27}Al/^{24}Mg$ at $\mu^{26}Mg^* = 22.2 \pm 1.4$ ppm, whereas CI chondrites define a $\mu^{26}Mg^*$ value of 4.5 ± 1.0 ppm. Except where shown, the error bars are smaller than symbols. Regression parameters were calculated using the external reproducibility or internal precision, whichever is larger. Fo: forsterite.

temperature of forsterite (∼1300 K; Krot et al. 2009). AOAs are aggregational objects composed of ^{16}O-rich ($\Delta^{17}O \sim -25‰$) forsterite condensates and CAIs; they have avoided significant melting (MacPherson et al. 2005). The temperatures inferred for the formation region of CAIs and AOAs are expected to have been reached in the innermost part of the protoplanetary disk during the initial stages of the solar system formation (Tscharnuter et al. 2009; Ciesla 2010). Thus, CAIs and AOAs can be used collectively to define the initial $^{26}Al/^{27}Al$ ratio and initial Mg-isotope composition ($\mu^{26}Mg_0$) in this region of the protoplanetary disk.

Bulk analyses of four AOAs (E1s, E2s, E3s, E4s) and four CAIs of different types (one fine-grained spinel-rich (22E), one Type B (E48), and two Type As (E104, 31E)) from the Efremovka CV chondrite define a line with a slope of $(5.252 \pm 0.019) \times 10^{-5}$ and initial $\mu^{26}Mg_0$ value of -15.9 ± 1.4 ppm (Figures 1(b) and (c)). We also analyzed AOA material mantling the E48 and E104 inclusions (i.e., forsterite-rich accretionary rims; Krot et al. 2002). The physical relationship between forsterite-rich accretionary rims and CAIs and their identical ^{16}O-rich compositions indicate that both types of objects are formed in the same reservoir. The E48 and E104 forsterite-rich accretionary rims plot on the bulk CAI–AOA isochron (Figure 1(c)) thereby confirming the contemporaneous formation of these AOAs and CAIs and, therefore, the validity of collectively using these objects to define the initial $^{26}Al/^{27}Al$ ratio and $\mu^{26}Mg_0$ value of the CAI- and AOA-forming region. We interpret the bulk CAI–AOA line as an ^{26}Al–^{26}Mg isochron corresponding to the timing of Al/Mg fractionation prior to and/or during formation of the Efremovka CAIs and AOAs by evaporation, condensation, and evaporative melting. The error on the slope of this isochron corresponds to an age uncertainty of ∼4000 years, suggesting a very short duration of these fractionation events. We interpret the intercept of this isochron ($\mu^{26}Mg_0$) as representing the initial Mg-isotope composition of the solar system. The slope of the ^{26}Al–^{26}Mg isochron is in agreement with the canonical $^{26}Al/^{27}Al$ ratio of $(5.23 \pm 0.13) \times 10^{-5}$ inferred from bulk measurements of CAIs from the oxidized CV chondrite Allende (Jacobsen et al. 2008). The initial $\mu^{26}Mg_0$ value of -15.9 ± 1.4 ppm inferred from the Efremovka CAI–AOA isochron is significantly different from the value of −38 ppm predicted for a uniform distribution of ^{26}Al in the solar system (Figure 1).

The $\mu^{26}Mg^*$ value of the Efremovka CAI–AOA isochron at a solar $^{27}Al/^{24}Mg$ ratio of 0.101 is 22.2 ± 1.4 ppm. If the $\mu^{26}Mg_0$ and $(^{26}Al/^{27}Al)_0$ inferred from the CV CAIs and AOAs are representative of the entire solar system, then solar system materials preserving the solar $^{27}Al/^{24}Mg$ ratio are predicted to have an identical $\mu^{26}Mg^*$ value of ∼22 ppm. To test this prediction, we measured the bulk Mg-isotope compositions of three CI (Ivuna type) carbonaceous chondrites (Alais, Ivuna, and Orgueil), which are considered to be the most chemically pristine solar system materials: they have solar abundances of most elements as well as solar $^{27}Al/^{24}Mg$ ratio (Asplund et al. 2009). The bulk Mg-isotope compositions of CI chondrites have an average $\mu^{26}Mg^*$ value of 4.5 ± 1.0 ppm, which is significantly lower than the $\mu^{26}Mg^*$ value of 22.2 ± 1.4 ppm defined by the Efremovka CAI–AOA isochron at a solar $^{27}Al/^{24}Mg$ ratio (Figure 1(c)).

We also measured bulk Mg-isotope compositions and $^{27}Al/^{24}Mg$ ratios of one enstatite chondrite, four ordinary chondrites, one R-chondrite, one acapulcoite, two angrites, two ureilites, and one Martian shergottite. The meteorite samples from

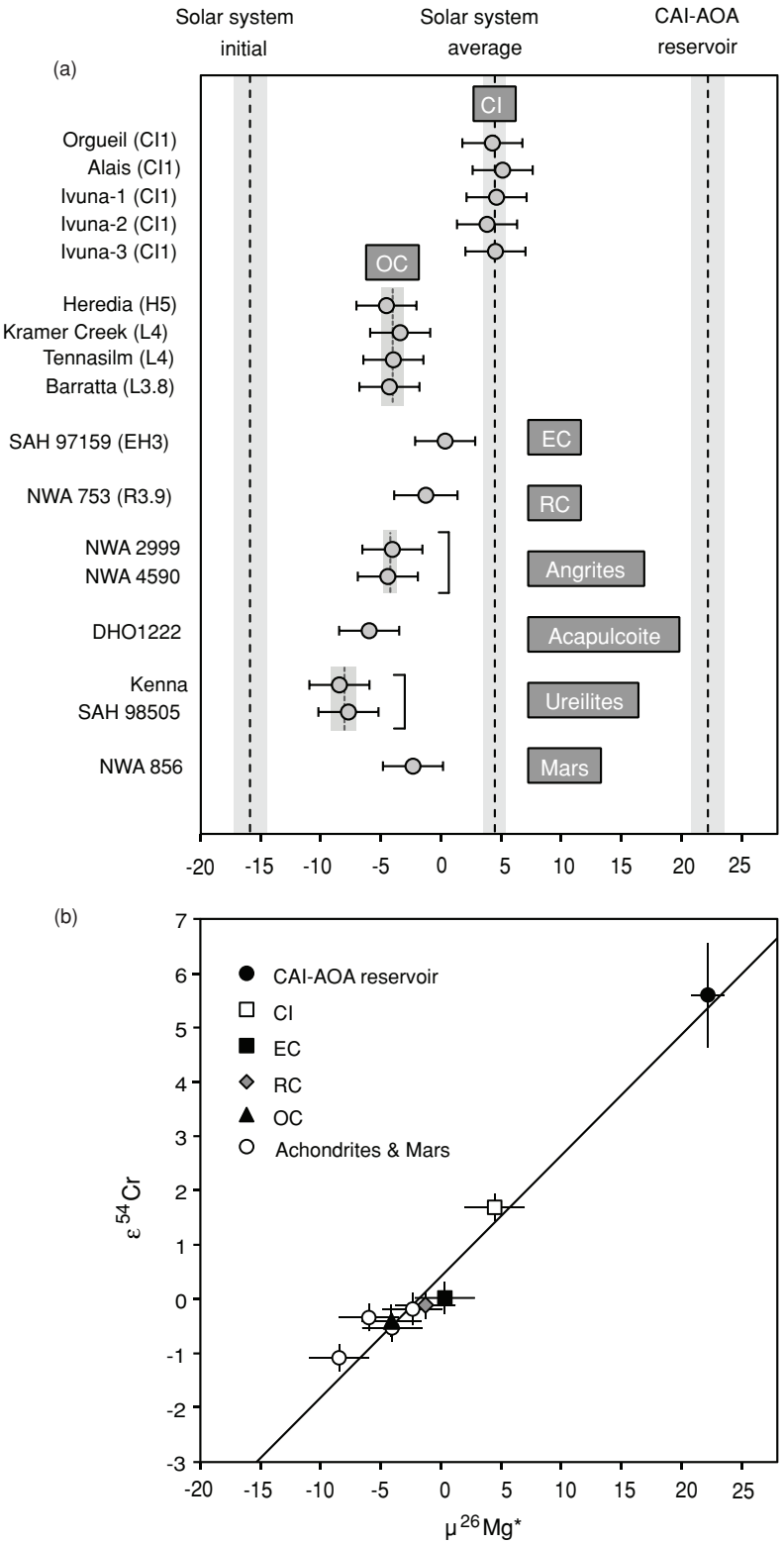

Figure 2. (a) μ^{26}Mg* values for primitive (chondritic) and differentiated asteroids and inner solar system planets. (b) Inner solar system μ^{26}Mg*–ϵ^{54}Cr correlation. ϵ^{54}Cr values are expressed as parts per 10,000 deviations from the terrestrial value. Error bars represent the external reproducibility or internal precision, whichever is larger.

differentiated asteroids analyzed here are believed to have formed >5 Myr after solar system formation (Amelin 2005, 2007; Goodrich et al. 2010). Thus, the bulk Mg-isotope compositions of these meteorites are not significantly affected by Al/Mg fractionation event(s) associated with their formation. None of the whole-rock Mg-isotope analyses of these meteorites approach the μ^{26}Mg* value of 22 ppm predicted by the CV CAI–AOA isochron and uniform distribution of ^{26}Al and μ^{26}Mg$_0$. Instead, these record μ^{26}Mg* values that are lower by 4–12 ppm compared to CI chondrites (Figure 2(a)).

Table 1
Mg and ^{54}Cr Isotope Composition of Inner Solar System Materials

Sample	Type of Material	^{27}Al/^{24}Mg	μ^{26}Mg*	μ^{25}Mg	μ^{26}Mg	N	ϵ^{54}Cr
31E	Bulk CAI	3.133 ± 0.016	1164.3 ± 2.7	5952 ± 18	12870 ± 41	10	6.80 ± 1.20
22E	Bulk CAI	3.336 ± 0.017	1244.8 ± 1.7	−2405 ± 7	−3454 ± 19	10	
E104	Bulk CAI	2.880 ± 0.058	1063.8 ± 4.0	−1031 ± 6	−950 ± 19	4	
E48 (1)	Bulk CAI	2.856 ± 0.057	1059.7 ± 3.5	12055 ± 14	24823 ± 29	5	
E48 (2)	Bulk CAI	2.674 ± 0.013	991.6 ± 4.1	10140 ± 9	20960 ± 22	6	
AR-E48	Fo-rich AR	0.03075 ± 0.0005	−5.6 ± 8.0	−1148 ± 18	−2239 ± 38	4	
AR-E104 (1)	Fo-rich AR	0.08501 ± 0.0013	21.6 ± 8.0	−1904 ± 9	−3696 ± 25	5	
AR-E104 (2)	Fo-rich AR	0.09237 ± 0.0014	23.8 ± 8.0	−2436 ± 31	−4735 ± 58	5	
E1s (1)	Bulk AOA	0.1100 ± 0.0006	26.2 ± 2.1	−1476 ± 8	−2855 ± 21	10	5.40 ± 0.40
E1s (2)	Bulk AOA	0.1330 ± 0.0007	33.2 ± 1.9	−1570 ± 11	−3029 ± 27	10	
E2s	Bulk AOA	0.3075 ± 0.0024	100.1 ± 3.6	−2465 ± 9	−4709 ± 21	7	
E3s	Bulk AOA	0.3686 ± 0.0018	120.4 ± 3.0	−1270 ± 9	−2355 ± 19	10	
E4s	Bulk AOA	0.0756 ± 0.0004	16.1 ± 3.2	−29 ± 14	−32 ± 29	6	
Ivuna (1)	CI	0.0977 ± 0.0004	4.6 ± 1.8	−147 ± 8	−276 ± 21	10	1.69 ± 0.25
Ivuna (2)	CI		3.8 ± 1.0	−136 ± 9	−258 ± 21	10	
Ivuna (3)	CI		4.5 ± 2.3	−109 ± 10	−200 ± 22	10	
Orgueil	CI	0.1030 ± 0.0005	4.3 ± 2.2	−143 ± 6	−277 ± 12	10	
Alais	CI	0.0988 ± 0.0005	5.1 ± 2.4	−143 ± 5	−276 ± 10	10	
SAH 97159	EC	0.0852 ± 0.0004	0.3 ± 1.9	−130 ± 17	−250 ± 37	50	
NWA 753	RC	0.0977 ± 0.0005	−1.3 ± 2.3	−159 ± 15	−298 ± 31	9	−0.11 ± 0.25
NWA 856	Mars	0.596 ± 0.003	−2.3 ± 1.8	−134 ± 6	−258 ± 18	10	
Kramer Creek	OC	0.0856 ± 0.0004	−3.4 ± 1.7	−183 ± 8	−355 ± 20	10	
Tennasilm	OC	0.0811 ± 0.0004	−4.0 ± 1.2	−157 ± 13	−308 ± 23	10	
Barratta	OC	0.0869 ± 0.0004	−4.3 ± 1.7	−172 ± 6	−333 ± 18	10	
Heredia	OC	0.0819 ± 0.0004	−4.5 ± 2.1	−162 ± 8	−314 ± 21	10	
NWA2999	Angrite	0.505 ± 0.003	−4.1 ± 1.7	−4 ± 12	−5 ± 27	10	−0.53 ± 0.25
NWA4590	Angrite	2.72 ± 0.01	−4.4 ± 2.0	−147 ± 11	−285 ± 24	10	
DHO1222	Acapulcoite	0.0878 ± 0.0004	−6.0 ± 1.3	−129 ± 8	−251 ± 21	10	−0.34 ± 0.25
Kenna	Ureilite	0.0059 ± 0.0001	−8.5 ± 1.1	−92 ± 8	−180 ± 22	10	−1.08 ± 0.25
SAH98505	Ureilite	0.0113 ± 0.0002	−7.7 ± 1.6	−101 ± 10	−199 ± 25	10	

Notes. Analytical uncertainties for the μ^{26}Mg*, μ^{25}Mg, and μ^{26}Mg values are quoted at the 2se level. For the ϵ^{54}Cr measurements, acquired following techniques outlined in Trinquier et al. (2008), the uncertainty reported is the external reproducibility of 25 ppm or internal error, whichever is larger. For the enstatite and ordinary chondrites as well as for the Martian shergottite, we used the values of Trinquier et al. (2007) obtained for the same meteorite groups. AR: accretionary rim; Fo: forsterite; EC: enstatite chondrite; OC: ordinary chondrite; RC: R-chondrite; *N*: number of acquisitions.

3. SIGNIFICANCE OF THE μ^{26}Mg* HETEROGENEITY

It is possible that the elevated μ^{26}Mg* value of 22.2 ± 1.4 ppm at the solar ^{27}Al/^{24}Mg ratio defined by the CAI–AOA regression reflects a pre-history of elevated ^{27}Al/^{24}Mg ratio for the CAI- and AOA-forming reservoir as a whole. Although evaporation and condensation processes can fractionate Al from Mg, the mineralogy and bulk chemistry of CAIs and AOAs are consistent with formation in a region with approximately solar composition (Grossman et al. 2000). Even allowing for a 15% increase in the ^{27}Al/^{24}Mg ratio of the CAI-forming region relative to the solar value requires timescales in the order of 1.5 Myr to produce the offset of 22.2 ± 1.4 ppm in CAIs and AOAs. Such an extended pre-history of the CAI- and AOA-forming reservoir is absent from the meteorite record and is inconsistent with the brief interval of ∼4000 years for the formation of these objects. Likewise, the observed variations in μ^{26}Mg* values of chondritic meteorites cannot be uniquely explained by Al/Mg fractionation events. For example, R and CI chondrites have nearly identical ^{27}Al/^{24}Mg ratios (Table 1), yet their μ^{26}Mg* values are different by 5.9 ± 2.6 ppm. Similarly, only 2.6 ppm of the observed 8.6 ± 1.4 ppm difference between the average μ^{26}Mg* values of the CI and ordinary chondrites could be attributed to Al/Mg fractionation given the difference in their ^{27}Al/^{24}Mg ratios. Thus, we rule out a pre-history of elevated ^{27}Al/^{24}Mg in the CAI–AOA-forming reservoir and Al/Mg fractionation events to account for the μ^{26}Mg* heterogeneity.

Large-scale nucleosynthetic isotopic heterogeneity exists among inner solar system solids, planets, and asteroids, most noticeably for neutron-rich isotopes of the iron-group elements such as ^{48}Ca, ^{50}Ti, ^{54}Cr, and ^{64}Ni (Birck 2004), and are interpreted as reflecting heterogeneous distribution of presolar components in the solar protoplanetary disk (Rotaru et al. 1992; Trinquier et al. 2007). Two views are considered for the origin of the solar system's ^{54}Cr heterogeneity: an ancient galactic component dominated by input from rare type Ia supernovae (Clayton 2003; Meyer et al. 1996) or, alternatively, heterogeneous seeding of the nascent solar system from a recent event, possibly a nearby massive star (Dauphas et al. 2010; Qin et al. 2011). The excesses and deficits in μ^{26}Mg* we find for primitive and differentiated meteorites as well as for the bulk CAI–AOA reservoir correlate with the ^{54}Cr abundance for the same samples or meteorite groups (Figure 2(b)). The preservation of a correlation between μ^{26}Mg* and ^{54}Cr suggests that the majority of the μ^{26}Mg* variability can be ascribed to a single cause: either ^{26}Al heterogeneity in the precursor material of the various solar system reservoirs or nucleosynthetic Mg-isotope heterogeneity unrelated to the decay of ^{26}Al. Although Mg-isotope anomalies of nucleosynthetic origin were reported in rare ^{26}Al-poor

Table 2
Initial $^{26}Al/^{27}Al$ Ratios of Bulk Solar System Reservoirs

Reservoir/Parent Body	$\mu^{26}Mg^*$	$(^{26}Al/^{27}Al)_0$
CV CAI- and AOA-forming reservoir	22.2 ± 1.4	$(5.25 \pm 0.02) \times 10^{-5}$
CI chondrite PB	4.5 ± 1.1	$(2.81 \pm 0.30) \times 10^{-5}$
Enstatite chondrite PB	0.3 ± 1.9	$(2.24 \pm 0.38) \times 10^{-5}$
Ordinary chondrite PB	-4.1 ± 1.2	$(1.63 \pm 0.25) \times 10^{-5}$
Angrite PB	-4.2 ± 1.7	$(1.61 \pm 0.32) \times 10^{-5}$
Ureilite PB	-8.1 ± 1.7	$(1.08 \pm 0.29) \times 10^{-5}$

Notes. The $\mu^{26}Mg^*$ and initial $^{26}Al/^{27}Al$ values of the CAI–AOA reservoir were calculated from the isochron relationship of Figure 1(b). For primitive and differentiated parent bodies, the $\mu^{26}Mg^*$ values are the averages and associated uncertainties (2 sd) of the samples representing individual meteorite groups. The $(^{26}Al/^{27}Al)_0$ values are calculated as deviations from the CAI–AOA value, assuming that all reservoirs are formed from the solar $^{27}Al/^{24}Mg$ ratio. PB, parent body.

Table 3
U-isotope Composition of the SAH99555 Angrite

Sample	Type of Material	$^{238}U/^{235}U$
SAH99555	Angrite	137.791 ± 0.011
BHVO-2 (a)	Terrestrial basalt	137.798 ± 0.011
BHVO-2 (b)	Terrestrial basalt	137.797 ± 0.011

Notes. U-isotope measurements were acquired by HR-MC-ICPMS based on protocols outlined in Weyer et al. (2008), and reported relative to CRM112a ($^{238}U/^{235}U = 137.844$; Condon et al. 2010). Two sample digestions of the BHVO-2 rock standard yielded identical $^{238}U/^{235}U$ values to that previously reported by Weyer et al. (2008). Uncertainties represent the external reproducibility.

inclusions (Sahijpal & Goswami 1998), mass balance calculations indicate that the potential presence of these anomalous components in chondritic meteorites will not affect their bulk Mg-isotope composition beyond the resolution of our analyses. Contrary to ^{54}Cr, which has multiple nucleosynthetic origins (Clayton 2003; The et al. 2007), all three Mg isotopes are coproduced during hydrostatic nucleosynthesis in massive stars (Arnett & Thilelemann 1985; Thilelemann & Arnett 1985), with the production of ^{25}Mg and ^{26}Mg increasing with stellar metallicity (Woosley & Weaver 1995). Therefore, if the solar system's ^{54}Cr heterogeneity represents an old, galactically inherited component, then preservation of a simple binary mixing relationship between $\mu^{26}Mg^*$ and $\epsilon^{54}Cr$ is difficult to reconcile with widespread Mg-isotope heterogeneity as the main source of variability in $\mu^{26}Mg^*$.

In contrast to the solar system's bulk Mg-isotope composition, the initial $^{26}Al/^{27}Al$ recorded by the Efremovka CAIs and AOAs cannot be explained by the expected contribution from the background abundances of ^{26}Al in the galaxy (Huss et al. 2009). This requires an input of freshly synthesized stellar material prior to or during the collapse of the protosolar molecular cloud to account for the totality of the solar system's inventory of ^{26}Al. Given that the massive stars that synthesize ^{26}Al also produce copious amounts of ^{54}Cr compared to the remaining Cr isotopes (The et al. 2007), the correlation we report in Figure 2(b) is most easily understood if it reflects variable incorporation of debris from a nearby stellar event that produced and delivered ^{26}Al and ^{54}Cr to the nascent solar system or, alternatively, contamination of the protosolar molecular cloud by a previous generation(s) of massive stars. This is consistent with the discovery of ^{54}Cr-rich grains of supernova origin in primitive meteorites (Dauphas et al. 2010; Qin et al. 2011). Because the Mg-isotope composition of supernova ejecta can be highly variable (Gyngard et al. 2010), it is possible that the $\mu^{26}Mg^*$ heterogeneity reported here represents the cumulative effect of both Mg-isotope and ^{26}Al heterogeneity. However, it is unclear how a late addition of freshly synthesized stellar material to the nascent solar system would result in a homogeneous distribution of ^{26}Al, but a heterogeneous distribution of Mg isotopes. As such, the discovery of widespread $\mu^{26}Mg^*$ heterogeneity in solar system objects is a highly significant finding, as it requires that some—if not all—of the $\mu^{26}Mg^*$ variability can be attributed to ^{26}Al heterogeneity. Although quantifying the extent of ^{26}Al heterogeneity solely based on our Mg-isotope measurements is difficult, we note that the magnitude of the $\mu^{26}Mg^*$ heterogeneity observed across solar system reservoirs (30.3 ± 1.8 ppm) is within the range of expected variations resulting from ^{26}Al heterogeneity (up to 38 ppm).

4. TESTING FOR ^{26}Al HETEROGENEITY IN THE SOLAR PROTOPLANETARY DISK

If the totality of the $\mu^{26}Mg^*$ variability is related to ^{26}Al heterogeneity, it is possible to estimate the initial ^{26}Al abundance in the accretion regions of asteroids and planets by comparing their present-day $\mu^{26}Mg^*$ with the initial $\mu^{26}Mg_0$ defined by the CAI–AOA isochron and its intercept at the solar $^{27}Al/^{24}Mg$ ratio. In Table 2, we show that if this assumption is valid, then large-scale heterogeneity—up to 80% reduction of the canonical $^{26}Al/^{27}Al$ ratio—may have existed throughout the inner solar system. The CI chondrites record an initial $^{26}Al/^{27}Al$ ratio of $\sim 2.8 \times 10^{-5}$, that is, approximately 54% of the value defined by Efremovka CAIs and AOAs. Thus, the CV CAI- and AOA-forming reservoir was characterized by an enhanced initial abundance of ^{26}Al compared to the average value of solar system material defined by CI chondrites, whereas the accretion regions of the terrestrial planets, ordinary chondrites, angrites, acapulcoites, and ureilites record variable depletions in ^{26}Al.

Rigorously testing whether the $\mu^{26}Mg^*$ variability primarily reflects ^{26}Al heterogeneity can be achieved by comparing high-precision U–Pb and ^{26}Al–^{26}Mg ages of pristine solar system materials, given that the U–Pb chronometer provides absolute ages that are free from assumptions of parent nuclide homogeneity. The validity of this approach, however, requires that both the U–Pb and ^{26}Al–^{26}Mg chronometers date the same event. We focus our discussion on the age difference between the CAI SJ101 (Amelin et al. 2011) and the SAH99555 angrite (Connelly et al. 2008b). SJ101 is the only CAI dated by the Pb–Pb method for which the U-isotope composition has been measured and currently defines the absolute age of CAIs. The SAH99555 angrite is one of the most pristine basaltic meteorites and has been dated via both the Pb–Pb and ^{26}Al–^{26}Mg methods by a number of groups (Connelly et al. 2008b; Amelin 2008; Schiller et al. 2010). Given the lack of U data for this meteorite, we measured the U-isotope composition of SAH99555 by HR-MC-ICPMS (Table 3). Based on the U–Pb system, we calculate an age difference of 3.57 ± 0.54 Myr between the formation of SJ101 and crystallization of SAH99555, which is not compatible with the age difference of $5.02^{+0.15}_{-0.13}$ Myr inferred from the ^{26}Al–^{26}Mg system for these two objects. Given the short duration of the CAI-forming process inferred from our study and the consistency in the Pb–Pb age of the SAH99555 meteorite obtained by different studies (Connelly et al. 2008b; Amelin 2008), it is unlikely that this age difference reflects

selective disturbance of the isotopic chronometers. Rather, it is consistent with our proposal that the CAI-forming reservoir was characterized by an enhanced abundance of ^{26}Al compared to the accretion region of the angrite parent body. To reconcile the mismatch between the U–Pb and ^{26}Al–^{26}Mg ages of SJ101 and SAH99555, the initial abundance of ^{26}Al in the accretion region of the angrite parent body is required to be reduced by 57%–85% of the ^{26}Al/^{27}Al value present in the CAI-forming reservoir, considering the uncertainties of the U–Pb ages. This is consistent with our independent estimate of 69% based on the Mg isotopes, which corresponds to an initial ^{26}Al/^{27}Al of $\sim 1.6 \times 10^{-5}$ for the angrite parent body and relative ^{26}Al–^{26}Mg age of 3.78 $\pm$ 0.23 Myr for SAH99555, and is in excellent agreement with its U–Pb age. We conclude that the bulk of the μ^{26}Mg* variability documented here reflects heterogeneity in the abundance of ^{26}Al across the solar protoplanetary disk at the time of CAI formation.

5. EARLY SOLAR SYSTEM PROCESSES AND THEIR CHRONOLOGY

Covariations in ^{54}Cr and ^{50}Ti among inner solar system objects have been ascribed to thermal processing of molecular cloud material, which resulted in preferential loss by sublimation of thermally unstable and isotopically anomalous presolar carriers, producing residual isotopic heterogeneity (Trinquier et al. 2009). The initial abundances of ^{26}Al in solar system reservoirs determined here resonate with their ^{54}Cr composition, suggesting that the ^{26}Al heterogeneity may have been established in a comparable way. This is consistent with a late-stage pollution of the nascent solar system from supernova debris as suggested by the μ^{26}Mg*–ϵ^{54}Cr correlation, but only if this occurred prior to the collapse of the protosolar molecular cloud. Thus, we propose that the ^{26}Al heterogeneity in solar system objects reflects variable degrees of thermal processing of their precursor material, probably associated with volatile-element depletions in the inner solar system. In this view, CAIs and AOAs represent samples of the complementary gaseous reservoir enriched in ^{26}Al by thermal processing, which resulted in the widespread ^{26}Al depletions observed among the inner solar system bodies. This implies the existence of a presolar carrier enriched in ^{26}Al among solar system materials, perhaps a presolar silicate, inherited from the protosolar molecular cloud.

The observation of ^{26}Al heterogeneity in the solar protoplanetary disk suggests that the ^{26}Al–^{26}Mg system cannot be readily used to deduce accurate chronologies of solar system events. Thus, current models for the formation and earliest evolution of our solar system based on the ^{26}Al–^{26}Mg chronometer require important revision. For example, the so-called canonical ^{26}Al/^{27}Al ratio of $\sim 5.2 \times 10^{-5}$ is typically used to infer the nature of the stellar source that delivered ^{26}Al to the nascent solar system (Meyer 2005). However, our results suggest that the solar system's initial ^{26}Al inventory is best approximated by the ^{26}Al/^{27}Al ratio of $\sim 2.8 \times 10^{-5}$ defined by CI chondrites (Table 1). A reduced initial abundance of ^{26}Al among some solar system reservoirs may impact the role of this radionuclide as a heat source for asteroid differentiation. However, we note that, assuming no heat loss and accretion contemporaneous with CAI formation, the amount of energy resulting from the decay of ^{26}Al in a body with a $(^{26}\mathrm{Al}/^{27}\mathrm{Al})_0$ ratio of 1×10^{-5} is ~ 1.2 kJ g^{-1}, which is 75% of the energy required to completely melt a chondritic body (Hevey & Sanders 2006); this would lead to the formation of an asteroid-wide magma ocean.

The existing ^{26}Al–^{26}Mg data for chondrules from unequilibrated ordinary chondrites (UOCs) require an age gap of $\sim$1.5 Myr between the formation of CAIs and chondrules (Kurahashi et al. 2008), assuming a uniform distribution of ^{26}Al in the solar system at the value of $\sim 5.2 \times 10^{-5}$. Recalculating the ^{26}Al–^{26}Mg ages of the UOCs' chondrules using the initial ^{26}Al/^{27}Al ratio of $\sim 1.6 \times 10^{-5}$ inferred for the accretion region of ordinary chondrites (Table 1) reduces the gap and suggests that ordinary chondrite chondrule formation started almost contemporaneously with the CV CAIs and AOAs. Thus, chondrule formation may have been a punctuated, recurrent process active during the entire life span of the solar protoplanetary disk.

REFERENCES

Amelin, Y. 2005, Science, 310, 839
Amelin, Y. 2007, Lunar Planet. Sci., 38, 2443
Amelin, Y. 2008, Geochim. Cosmochim. Acta, 72, 4874
Amelin, Y., Kaltenbach, A., Iizuka, T., Stirling, C. H., Ireland, T. R., Petaev, M., & Jacobsen, S. B. 2011, Earth Planet. Sci. Lett., 300, 343
Amelin, Y., Krot, A. N., Hutcheon, I. D., & Ulyanov, A. A. 2002, Science, 297, 1678
Arnett, W. D., & Thilelemann, F.-K. 1985, ApJ, 295, 589
Asplund, M., Grevesse, N. J., Sauval, A., & Scott, P. 2009, ARA&A, 47, 481
Birck, J.-L. 2004, Rev. Mineral. Geochem., 55, 25
Bizzarro, M., Baker, J. A., & Haack, H. 2004, Nature, 431, 275
Bizzarro, M., Paton, C., Larsen, K., Schiller, M., Trinquier, A., & Ulfbeck, D. 2011, J. Anal. At. Spectrom., 26, 565
Brennecka, G. A., et al. 2010, Science, 327, 449
Ciesla, F. J. 2010, Icarus, 208, 455
Clayton, D. D. 2003, Handbook of Isotopes in the Cosmos: Hydrogen to Gallium (Cambridge: Cambridge Univ. Press)
Condon, D. J., McLean, N., Noble, S. R., & Bowring, S. A. 2010, Geochim. Cosmochim. Acta, 74, 7127
Connelly, J. N., Amelin, Y., Krot, A. N., & Bizzarro, M. 2008a, ApJ, 675, L121
Connelly, J. N., Bizzarro, M., Thrane, K., & Baker, J. A. 2008b, Geochim. Cosmochim. Acta, 72, 4813
Dauphas, N., et al. 2010, ApJ, 655, 1577
Galy, A., Young, E. D., Ash, R. D., & O'Nions, R. K. 2000, Science, 290, 1751
Goodrich, C. A., Hutcheon, I. D., Kita, N. T., Huss, G. R., Cohen, B. A., & Keil, K. 2010, Earth Planet. Sci. Lett., 295, 531
Goswami, J. N. 2004, New Astron. Rev., 48, 125
Grossman, L., Ebel, D. S., Simon, S. B., Davis, A. M., Richter, F. M., & Parsad, N. M. 2000, Geochim. Cosmochim. Acta, 64, 2879
Gyngard, F., Zinner, E., Nittler, L. R., Morgand, A., Stadermann, F. J., & Hynes, M. 2010, ApJ, 717, 107
Hevey, P. J., & Sanders, S. 2006, Meteorit. Planet. Sci., 41, 95
Huss, G. R., Meyer, B. S., Srinivasan, G., Goswami, J. N., & Sahijpal, S. 2009, Geochim. Cosmochim. Acta, 73, 4922
Jacobsen, B., et al. 2008, Earth Planet. Sci. Lett., 272, 353
Krot, A. N., Mckeegan, K. D., Leshin, L. A., MacPherson, G. J., & Scott, E. R. D. 2002, Science, 295, 1051
Krot, A. N., et al. 2009, Geochim. Cosmochim. Acta, 73, 4963
Kurahashi, E., Kita, N. T., Nagahara, H., & Morishita, Y. 2008, Geochim. Cosmochim. Acta, 72, 3865
Lee, T., Papanastassiou, D. A., & Wasserburg, G. J. 1977, ApJ, 211, L107
MacPherson, G. J. 2003, in Treatise on Geochemistry, ed. H. D. Holland, K. K. Turekian, & A. M. Davis (Meteorites, Comets and Planets, Vol. 1; Oxford: Pergamon), 201
MacPherson, G. J., Simon, S. B., Davis, A. M., Grossman, L., & Krot, A. N. 2005, in ASP Conf. Ser. 341, Chondrites and the Protoplanetary Disk, ed. A. N. Krot, E. R. D. Scott, & B. Reipurth (San Francisco, CA: ASP), 225
McKeegan, K. D., & Davis, A. M. 2003, in Treatise on Geochemistry, ed. H. D. Holland, K. K. Turekian, & A. M. Davis (Meteorites, Comets and Planets, Vol. 1; Oxford: Pergamon), 431
Meyer, B. S. 2005, in ASP Conf. Ser. 341, Chondrites and the Protoplanetary Disk, ed. A. N. Krot, E. R. D. Scott, & B. Reipurth (San Francisco, CA: ASP), 515
Meyer, B. S., Krishnan, T. D., & Clayton, D. D. 1996, ApJ, 462, 825
Paton, C., et al. 2011, J. Anal. At. Spectrom., submitted
Qin, L., Nittler, L. R., Alexander, C. M. O'D, Wang, J., Stadermann, F. J., & Carlson, R. W. 2011, Geochim. Cosmochim. Acta, 75, 629

Rotaru, M., Birck, J.-L., & Allègre, C. J. 1992, Nature, 358, 465
Russell, S. S., Srinivasan, G., Huss, G. R., Wasserburg, G. J., & MacPherson, G. J. 1996, Science, 273, 757
Sahijpal, S., & Goswami, J. N. 1998, ApJ, 509, L137
Schiller, M., Baker, J. A., & Bizzarro, M. 2010, Geochim. Cosmochim. Acta, 74, 4844
The, L.-S., El Eid, M. F., & Meyer, B. S. 2007, ApJ, 655, 1058
Thilelemann, F.-K., & Arnett, W. D. 1985, ApJ, 295, 604
Thrane, K., Bizzarro, M., & Baker, J. A. 2006, ApJ, 646, L159
Trinquier, A., Birck, J.-L., & Allègre, C. J. 2007, ApJ, 655, 1179
Trinquier, A., Birck, J.-L., & Allègre, C. J. 2008, J. Anal. At. Spectrom., 23, 1565
Trinquier, A., Elliott, T., Ulfbeck, D., Coath, C., Krot, A. N., & Bizzarro, M. 2009, Science, 324, 374
Tscharnuter, W. M., Schönke, J., Gail, H.-P., Trieloff, M., & Lüttjohann, E. 2009, A&A, 504, 109
Villeneuve, J., Chaussidon, L., & Libourel, G. 2009, Science, 325, 985
Weyer, S., Anbar, A. D., Gerdes, A., Gordon, G. W., Algeo, T. J., & Boyle, E. A. 2008, Geochim. Cosmochim. Acta, 72, 345
Woosley, S. E., & Weaver, T. A. 1995, ApJS, 101, 181